Supporting Information

Adaptive remodeling of skeletal muscle energy metabolism in high-altitude hypoxia: Lessons from AltitudeOmics

Adam J. Chicco[1,2*], Catherine H. Le[2], Erich Gnaiger[3], Hans C. Dreyer[4], Jonathan B. Muyskens[4], Angelo D'Alessandro[5], Travis G. Nemkov[5], Austin D. Hocker[4], Jessica E. Prenni[6], Lisa M. Wolfe[6], Nathan M. Sindt[6], Andrew T. Lovering[5], Andrew W. Subudhi[7], Robert C. Roach[8]

SI Materials and Methods

Subjects and AltitudeOmics project. Subjects (7 male, 7 female; 21 ± 2 years of age) were a sub-set of 21 individuals studied at SL (Eugene, Oregon, USA) and following 16 days of acclimatization to 5260 m (A16) on Mt. Chacaltaya in the Bolivian Andes during the 2012 AltitudeOmics project (1). Data pertaining to select physical characteristics of these subjects have been previously reported (2-7). In addition, investigations of erythrocyte metabolism during and following high-altitude hypoxia in these subjects have recently been published elsewhere (8-11). The present study is the first report of any skeletal muscle analyses from the AltitudeOmics project, and represents an entirely unique investigation of this 14-subject cohort. All subjects engaged in light voluntary activity and were provided ad libitum meals and lodging to minimize confounding effects of negative energy balance and inactivity. All procedures conformed to the Declaration of Helsinki and were approved by the Universities of Colorado, Oregon, and Utah Institutional Review Boards and the U.S. Department of Defense Human Research Protection Program Office.

Skeletal Muscle Sampling and Handling. Muscle biopsies were obtained under resting post-absorptive conditions at least 48 hours following any rigorous exercise or testing, with daily protocol and timing matched as closely as possible for subjects at BL and A16. The medial vastus lateralis muscle was sampled as previously described (12) using the Bergström technique under local anesthesia (1% lidocaine s.c.). 100-150 mg samples were immediately sectioned with a sterile scalpel, and a portion either snap frozen and stored in liquid nitrogen or -80C freezers until biochemical analysis, or immediately placed into ice-cold biopsy preservation medium (BIOPS) containing (in mM) 10 Ca^{2+}-EGTA, 20 imidazole, 50 potassium-4-morpholinoethanesulfonic acid, 0.5 dithiothreitol, 6.56 $MgCl_2$, 5.77 ATP and 15 phosphocreatine at pH 7.1 for preparation of permeabilized fibers for mitochondrial respiration experiments.

Preparation of Permeabilized Muscle Fibers. Structurally sound muscle fiber bundles were selected from biopsies in ice-cold BIOPS, and mechanically separated while removing any visible adipose and connective tissue using fine forceps under a dissecting microscope. Teased fiber bundles (2-6 mg) were then transferred to BIOPS containing 50 μg/mL saponin for twenty minutes of permeablization of the sarcolemma while leaving the mitochondria and intracellular structures intact (13), followed by 3 x 10 min washes in ice-cold MiR06 respiration buffer containing (in mM) 0.5 EGTA, 3 $MgCl_2$, 60 K-lactobionate, 20 taurine, 10 KH_2PO_4, 20 HEPES, 110 sucrose, with 1 g/L fatty-acid free BSA and 2,800 U/mL catalase. Permeabilized fibers were carefully blotted on Whatman filter paper for 2-3 seconds to remove excess buffer, weighed and immediately placed in the Oxygraph chamber containing MiR06 at 37˚C for stabilization prior to respiration experiments described below.

Mitochondrial Respiration. Mitochondrial respiratory function was determined in permeabilized muscle fiber bundles using two Oxygraph-2k high-resolution respirometers (Oroboros Instruments, Innsbruck, Austria). Oxygen flux was monitored in real-time by resolving changes in the negative time derivative of the chamber oxygen concentration signal following standardized instrumental and chemical background calibrations using Datlab software (Oroboros Insturments, Innsbruck, Austria) performed daily (instrumental) or before every experiment (chemical background). All respirometry data were collected from chambers strictly maintained at 37˚C in a hyperoxygenated environment (275-400 μM) to avoid potential limitations in oxygen diffusion in permeabilized muscle fiber bundles (13,14). A detailed description of the respiration protocols and associated respiratory states generated by the sequential titration of each constituent are provided in Table S1. All samples were run in duplicate and averaged, and occasionally a third or fourth time if the response of repeats lacked uniformity. Any fiber preparations exhibiting a greater than 10% increase in flux in response to Cytochrome c (indicating loss of

outer mitochondrial membrane integrity) were excluded from analyses. Selected flux control ratios were calculated for determination of respiratory coupling/leak and substrate control as described in Supplemental Table S1.

Serum and muscle metabolomic profiling. Serum samples (10 µl) or muscle biopsies (10mg) were immediately extracted in ice-cold lysis/extraction buffer (methanol:acetonitrile:water 5:3:2) at 1:50 dilutions or 10mg tissue/ml buffer ratios. Samples were then agitated at 4°C for 30 min and then centrifuged at 10,000g for 15min at 4°C. Protein pellets were discarded, while supernatants and the methanol soluble lipid fraction were stored at -80°C prior to metabolomics analyses. Ten µl of sample extracts were injected into an UHPLC system (Vanquish, Thermo, San Jose, CA, USA) and run on a Kinetex XB-C18 column (150x2.1 mm i.d., 1.7 µm particle size) (Phenomenex, Torrance, CA, USA) over 9 minutes at 350 µl/min (mobile phase: 5% acetonitrile, 95% 18 mΩ H_2O, 0.1% formic acid). The UHPLC system was coupled online with a Q Exactive system (Thermo, San Jose, CA, USA), scanning in Full MS mode (2 µscans) at 70,000 resolution in the 60-900 m/z range (hydrophilic fraction) or 150 to 2000 m/z (hydrophobic fraction), 4kV spray voltage, 15 sheath gas and 5 auxiliary gas, operated in negative and then positive ion mode (four separate runs per sample). Calibration was performed before each analysis against positive or negative ion mode calibration mixes (Piercenet – Thermo Fisher, Rockford, IL, USA) to ensure sub ppm error of the intact mass. Metabolite assignments were performed using the software Maven (Princeton, NJ, USA), upon conversion of .raw files into .mzXML format through MassMatrix (Cleveland, OH, USA). The software allows for peak picking, feature detection and metabolite assignment against the KEGG pathway database. Assignments were further confirmed against chemical formula determination (as gleaned from isotopic patterns and accurate intact mass), and retention times against a >630 standard compounds library including commercially available glycolytic and Krebs cycle intermediates, amino acids, glutathione homeostasis and nucleoside phosphates (SIGMA Aldrich, St. Louis, MO, USA; IROATech, Bolton, MA, USA).

Muscle Proteomic profiling. Frozen muscle biopsy sections (~30mg) carefully pre-selected to be free of blood and connective tissue were thawed and immediately homogenized at 1:20 (w/v) in glass-glass tissue grinders containing to 50 mM Tris-HCl (pH 7.4), 150 mM NaCl, 1% SDS with a protease inhibitor cocktail (Roche) to solubilize proteins while preventing any proteolysis during preparation. Samples were sonicated 10 x 1 sec on ice following homogenization, left on ice for 30 min with occasional vortexing to ensure solubilization, then centrifuged at 14,000 g at 4C for 20 min to remove insoluble material. The supernatant was collected as assayed for total protein using the BCA assay and stored at -80C until analysis. Thirty micrograms of protein were aliquoted for peptide purification and concentrated using an on-line enrichment column (Thermo Scientific 5µm, 100 µm ID x 2cm C18 column). Subsequent chromatographic separation was performed on a reverse phase nanospray column (Thermo Scientific EASYnano-LC, 3µm, 75 µm ID x 100mm C18 column) using a 90 minute linear gradient from 10%-30% buffer B (100% ACN, 0.1% formic acid) at a flow rate of 400 nanoliters/min. Peptides were eluted directly into the mass spectrometer (Thermo Scientific Orbitrap Velos) and spectra were collected over a m/z range of 400-2000 Da using a dynamic exclusion limit of 2 MS/MS spectra of a given peptide mass for 30 s (exclusion duration of 90 s). The instrument was operated in Orbitrap-LTQ mode where precursor measurements were acquired in the orbitrap (60,000 resolution) and MS/MS spectra (top 20) were acquired in the LTQ ion trap with a normalized collision energy of 35kV. Compound lists of the resulting spectra were generated using Xcalibur 2.2 software (Thermo Scientific) with a S/N threshold of 1.5 and 1 scan/group.

Tandem Mass Tag (TMT) labeling of peptides is a MS/MS based analysis strategy for the relative quantification of proteins in complex samples. TMT tags are designed to differentially label identical peptides from different experimental samples. The analysis of each labeled sample can be multiplexed into a single analysis in which the differential relative abundance of each peptide can be measured with great accuracy. TMT labeling allows for the simultaneous determination of sequence identity of the peptide and relative abundance of peptide groups can be determined in each experimentally derived sample.

In this study, 14 human subjects were chosen for the proteomic analysis of hypoxia-induced changes in muscle tissue. Each subject had a baseline sample (normoxia) and a sample taken at altitude (hypoxia). The objective of proteomics work is to identify differentially abundant proteins under each experimental condition. We used Tandem Mass Tag labeling to allow for the multiplexing of sample groups such that up to 5 individuals per group (each with paired samples) could be analyzed simultaneously via LC-MS/MS to determine protein abundance changes in samples taken under Normoxic and Hypoxic conditions.

Labeling Procedure: Each individual sample was digested with trypsin and labeled with a unique reporter tag (TMT 10-Plex, Thermo Pierce). The group of 10 digested samples were combined into a single sample and subjected to offline UPLC-UV fractionation using high pH Reverse Phase. 36 fractions were collected and concatenated into 12 pools for analysis via LC-MS/MS .

LC-MS/MS data was searched against the human Uniprot protein database (www.uniprot.org) in MASCOT Server (v. 2.3). These data were imported into Scaffold Q+S (www.proteomesoftware.com) for data refinement and quantification of reporter tag intensity. All baseline samples in each of the three sample groups (I, II, III – n=5 persons each) are used as the reference sample. With a false discovery rate of peptides set at 0.1%, over 600 proteins were confidently identified (FDR < 1%).

DATABASE SEARCHING -- Tandem mass spectra were extracted, charge state deconvoluted and deisotoped by ProteoWizard (MS-Convert) version 3.0. All MS/MS samples were analyzed using Mascot (Matrix Science, London, UK; version 2.3.02). Mascot was set up to search the uniprot_hum_rev_011014 database (unknown version, 176946 entries) assuming the digestion enzyme trypsin. Mascot was searched with a fragment ion mass tolerance of 0.80 Da and a parent ion tolerance of 20 PPM. Oxidation of methionine and carbamidomethyl of cysteine were specified in Mascot as variable modifications.

CRITERIA FOR PROTEIN IDENTIFICATION-- Scaffold (version Scaffold_4.3.2, Proteome Software Inc., Portland, OR) was used to validate MS/MS based peptide and protein identifications. Peptide identifications were accepted if they could be established at greater than 79.0% probability to achieve an FDR less than 0.1% by the Scaffold Local FDR algorithm. Protein identifications were accepted if they could be established at greater than 99.0% probability and contained at least 2 identified peptides. Protein probabilities were assigned by the Protein Prophet algorithm (15). Proteins that contained similar peptides and could not be differentiated based on MS/MS analysis alone were grouped to satisfy the principles of parsimony.

QUALITY CONTROL- Instrument functionality and stability was monitored using the MassQC software (Proteome Software). This software uses a set of quantitative metrics developed by the National Institute of Science and Technology (NIST) in collaboration with the National Cancer Institute's Clinical Proteomic Technologies for Cancer (CPTC) that monitor technical variability in mass spectrometry-based proteomics instrumentation. Quality control samples containing a mixture of 6 trypsin digested bovine proteins were injected at least once every 24 hours throughout the analysis, and the data from this run was analyzed using the MassQC software. Values for all metrics were within normal limits throughout the duration of the experiment indicating instrument stability and data robustness.

ACKNOWLEDGEMENTS. This study was part of the AltitudeOmics project that explore the basic mechanisms controlling human acclimatization to hypoxia. Many people and organizations have invested enormous amounts of time and resources to make AltitudeOmics a success. Foremost, the study was made possible by the tireless support, generosity, and tenacity of our research subjects. AltitudeOmics principal investigators were A.T. Lovering, A.W. Subudhi, and R.C. Roach. A complete list of other investigators on this multinational, collaborative effort involved in development, subject management and data collection, supporting industry partners, and people and organizations in Bolivia that made AltitudeOmics possible is available in the first paper in this series (1). The authors are extremely grateful to J. Kern, J.E. Elliot, S.S. Laurie, and K.M. Beasley for their invaluable assistance in the blood gas data collection for this study. This study was supported by in part by U.S. Department of Defense Grants W81XWH-11-2-0040 TATRC to R.C. Roach and W81XWH-10-2-0114 to A.T. Lovering); the team at Oroboros Instruments, Innsbruck, Austria; the Mitochondrial Physiology Laboratory at Colorado State University; and by the Altitude Research Center and the Charles S. Houston Endowed Professorship, Department of Emergency Medicine, School of Medicine, University of Colorado Denver.

SI Figures and Tables

Figure S1

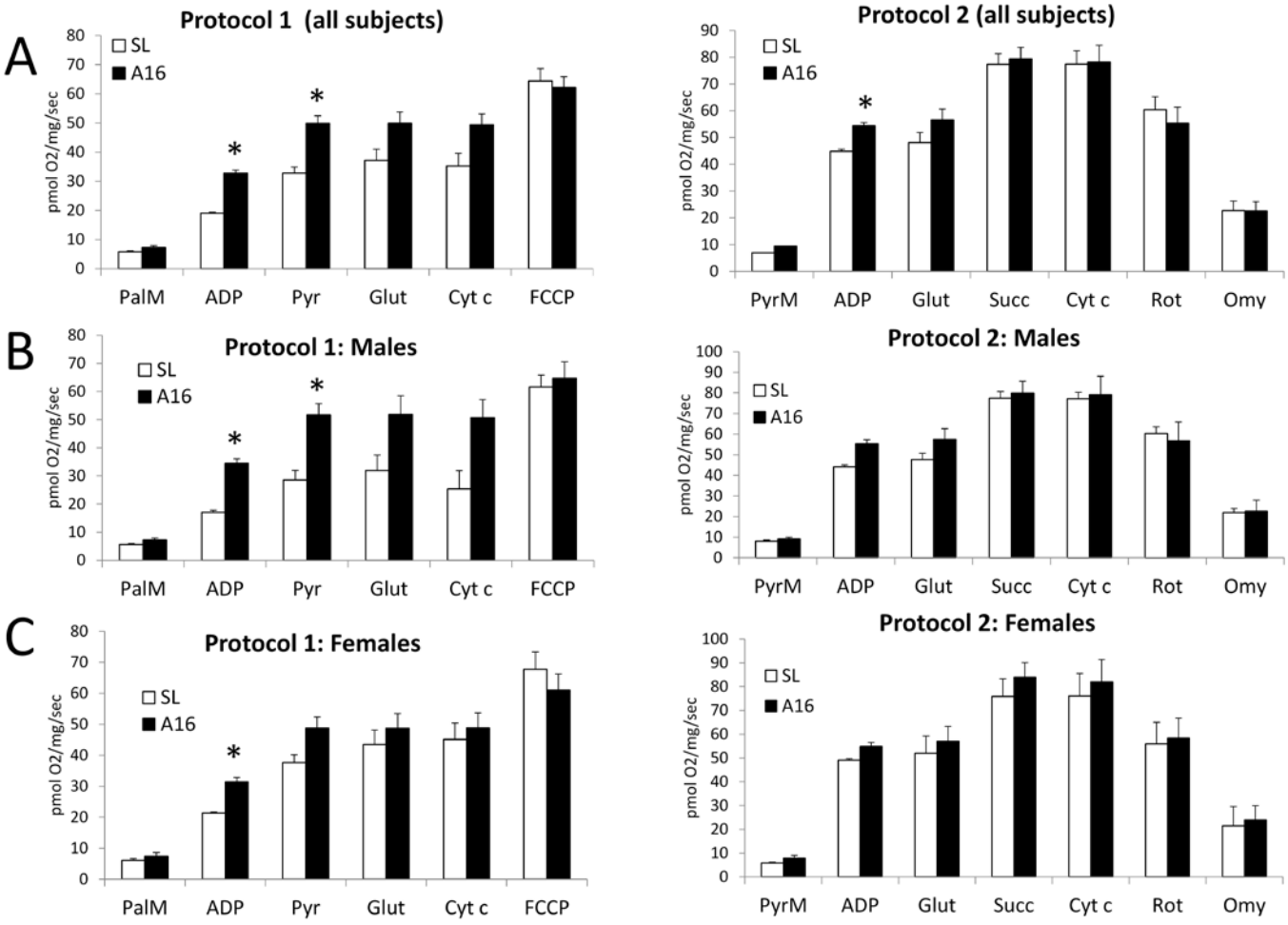

Supplemental Figure S1. Complete mean data from high resolution respirometry studies.
Graphs represent mass-corrected oxygen flux of permeabilized muscle fibers following each titration in Protocols 1 and 2, generating the cumulative respiratory states described in Table S1 for all subjects (n = 14; A), males (n = 7; B), and females (n = 7; C). Data are means ± SEM. *$P < 0.05$ for SL vs. A16 by paired *t*-test.

Figure S2

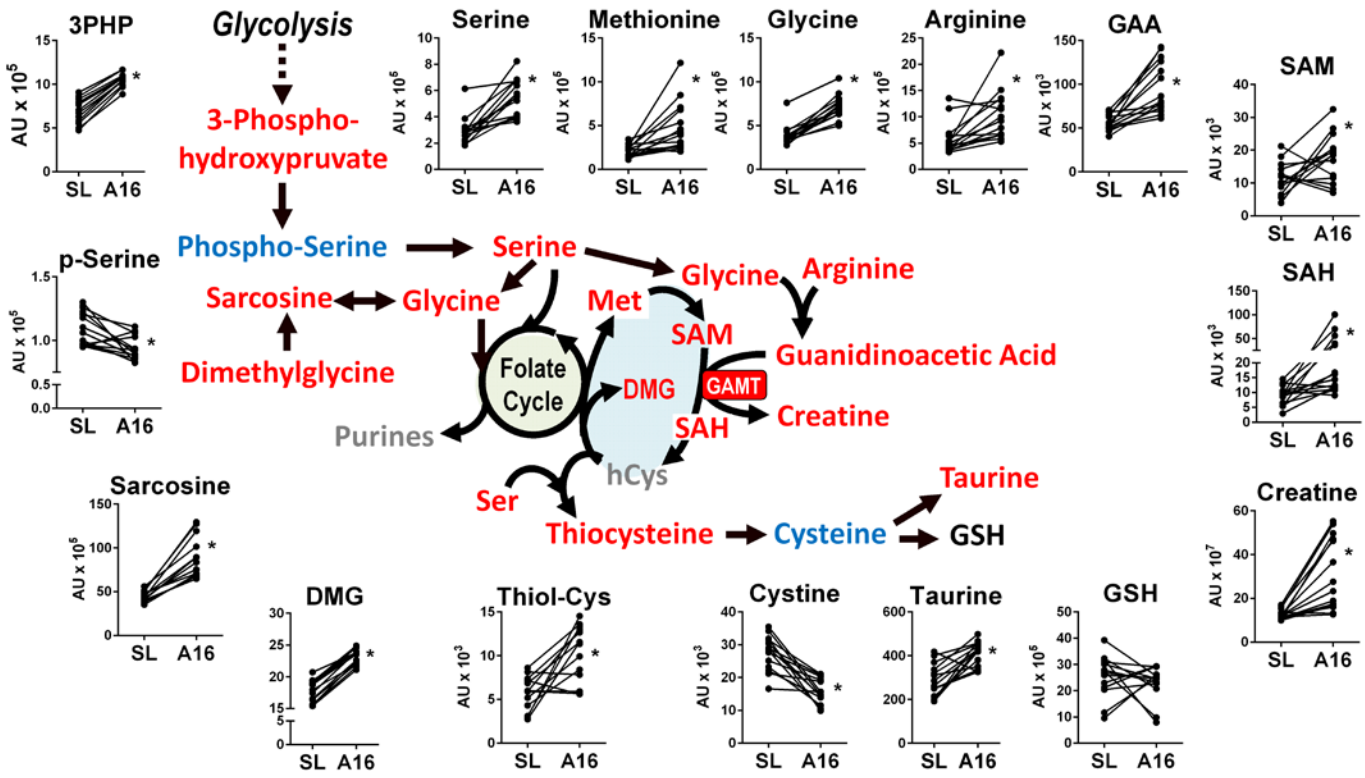

Supplemental Figure S2. Increased activity of muscle one-carbon metabolism pathways in hypoxia. Schematic illustrates one-carbon metabolism pathways fueled by *de novo* serine synthesis from glycolytic intermediate 3-phospho-hydroxypyruvate (3PHP), comprising the folate cycle (grey), methionine cycle (blue) and transsulphuration pathway (yellow). Metabolites depicted were found to increase (red font), decrease (blue font), or not change (black font) from SL to A16 ($q < 0.05$), or were undetected (grey font) by LC/MS. Guanidinoacetic acid methyltransferase (GAMT; red box) increased relative to CS at A16. Corresponding data for all detected metabolites at SL and A16 are shown in adjacent graphs. DMG, dimethylglycine; GAA, guanidinoacetic acid; GSH, glutathione; hCys, homocysteine; Met, methionine; SAH, S-adenosyl-homocysteine; SAM, S-adenosyl-methionine; Thiol-cys, thiol cysteine. *q< 0.05 vs. SL in FDR-adjusted paired t-tests.

Figure S3

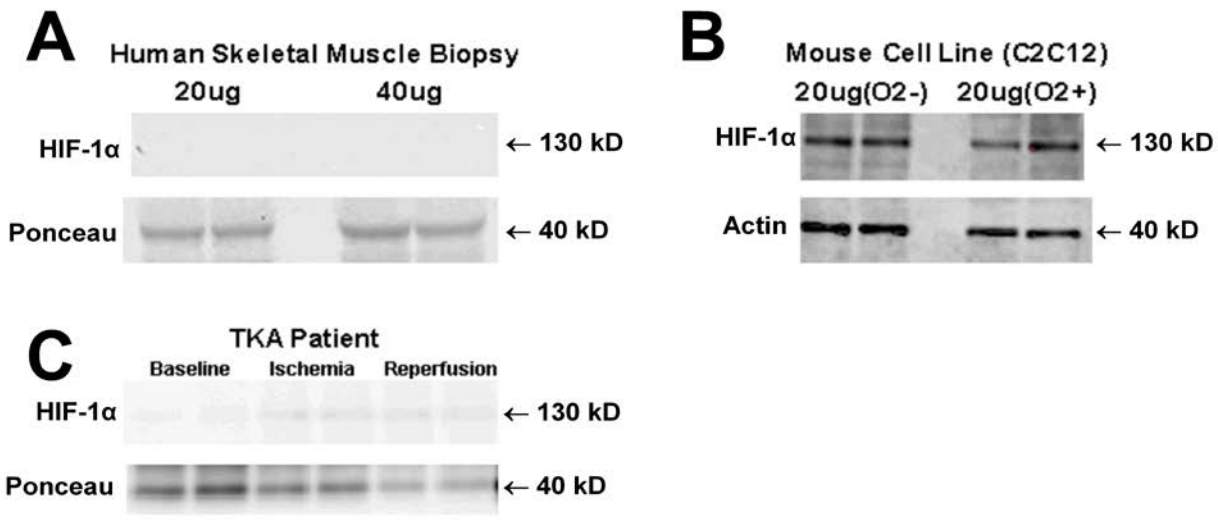

Supplemental Figure S3. Muscle HIF-1α protein expression. (A) HIF-1α protein was undetectable by Western blot of 20 and 40 µg muscle protein extracts from all study participants at SL or A16, despite successful membrane protein transfer evidenced by expected signals for actin at 40 kDa. **(B)** Validation of the antibody (Cell Signaling Cat# 3716S) was confirmed by robust signals in 20 µg protein extracts from C2C12 myoblasts cultured under anoxic conditions (O2-) that were slightly attenuated by culturing in 9% oxygen (O2+). **(C)** Further antibody validation was performed in human *vastus lateralis* muscle biopsies (20 µg protein) obtained from a patient undergoing total knee arthroplasty (TKA), demonstrating a detectable HIF-1α signal following ischemia induced by application of tourniquet to the upper leg, which was retained following 2 hours of reperfusion.

Supplemental Table S1. High resolution respirometry protocols and associated respiratory states and control factors assessed in muscle fiber mitochondrial respiration experiments

Protocol constituents (listed in order of titration)	**Abbrev.** (Fig S1)	**Respiratory State (common nomenclature);** Explanation
Protocol 1		
Palmitoylcarnitine + Malate (0.2 mM + 2 mM)	PalM	**Fatty Acid LEAK (FAO_L)**; Maximal respiration supported by high fatty acid and malate concentration, but no ADP; facilitated by the intrinsic rate of $\Delta\Psi_m$ dissipation (essentially proton leak) across the IMM
ADP (5 mM)	ADP	**Fatty acid OXPHOS (FAO_P)**; Maximal rate of OXPHOS-linked respiration supported by palmitoylcarnitine + malate oxidation in the presence of ADP
Pyruvate (5 mM)	Pyr	**$(FAO+PM)_P$;** Maximal rate of OXPHOS-linked respiration supported by palmitoylcarnitine + pyruvate and malate
Glutamate (10 mM)	Glut	**$(FAO+CI)_P$**; Maximal rate of OXPHOS-linked respiration supported by saturating concentrations of complex I (CI) substrates + palmitoylcarnitine and ADP
Cytochrome *c* (10 μM)	Cyt *c*	Test of outer mitochondrial membrane integrity (fully intact mitochondria give minimal response)
FCCP (1μM followed by 0.5μM titrations until maximal flux is reached)	FCCP	**$(FAO+CI)_E$**; Maximal mitochondrial respiratory (ETS) capacity supported by saturating concentrations of the preceding substrates + Cyt *c* (to supply electrons to CIV in any damaged mitochondria) and protonophore (FCCP) to remove any limitation of $\Delta\Psi_m$ on electron flow through the ETS
Protocol 2		
Pyruvate + Malate (5 mM + 2 mM)	PyrM	**Pyruvate LEAK (PM_L);** Maximal respiration supported by high pyruvate and malate concentration, but no ADP; facilitated by the intrinsic rate of $\Delta\Psi_m$ dissipation (essentially proton leak) across the IMM
ADP (5 mM)	ADP	**Pyruvate OXPHOS (PM_P)**; Maximal rate of OXPHOS-linked respiration supported by pyruvate + malate oxidation (in the presence of ADP)
Glutamate (10 mM)	Glut	**CI_P or N_P;** Maximal rate of OXPHOS-linked respiration supported by the preceding Complex I substrates in the absence of fatty acids
Succinate (10 mM)	Succ	**$(CI+II)_P$ or NS_P;** Maximal rate of OXPHOS-linked respiration supported by Complex I + II substrates (full TCA activity) in the absence of fatty acids
Cytochrome *c* (10 μM)	Cyt c	Test of outer mitochondrial membrane integrity (fully intact mitochondria give minimal response)
Rotenone (0.5 μM)	Rot	**Succinate OXPHOS (CII_P or S_P)**; Maximal rate of OXPHOS-linked respiration supported by preceding substrates + rotenone to block CI; revealing the unabated succinate (Complex II)-supported rate
Oligomycin A (0.5 μM)	Omy	**Succinate LEAK (CII_L or S_L)**; Maximal respiration supported by preceding titrations (Complex II) + the ATP synthase inhibitor oligomycin; pyruvate and malate concentration, but no ADP; facilitated by the intrinsic rate of $\Delta\Psi_m$ dissipation (essentially proton leak) across the IMM

Titrations are listed in the order they are added in the two respiratory protocols illustrated in Figure S2, generating the cumulative respiratory states described in the right column. Bolded respiratory states and control factors correspond to those in the main manuscript. See text and (14) for additional explanation and interpretation of respiratory states. Abbreviations not listed above: FCCP, carbonyl cyanide-4-(trifluoromethoxy)phenylhydrazone; CI/II, respiratory Complexes I/II. $\Delta\Psi_m$, mitochondrial membrane potential.

Supplemental Table S1 (cont.). Respiratory control factors derived from respirometry protocols

Control factor	Formula	Explanation
OXPHOS Coupling Control	$(CI+PalM)_{P/E}$	The proportion of maximal ETS capacity utilized during OXPHOS; assessed by dividing the flux after Glut in protocol 1 by the following rate induced by the addition of FCCP
OXPHOS Coupling Efficiency (CE)	$1- (X_L/X_P)$ or $(X_P/X_L)/X_P$	The proportion of OXPHOS (P; coupled) not accounted for by LEAK (L; uncoupled) respiration with the same substrate (X), where 1.0 is fully coupled respiration. Calculated as $(X_P /X_L)/X_P$ (or $1- (X_L/X_P)$) for a given substrate X using adjacent P and L states in the same protocol

Respiratory control factors calculated from respiratory states generated during titration protocols described above. Subscript "P" refers to an OXPHOS state (in presence of ADP), "L" to LEAK states (in absence of ADP or presence of oligomycin), and "E" to non-coupled states following addition of FCCP.

Supplemental Table S2a. Muscle proteomic profiling: all significant changes from SL to A16 expressed relative to total peptide (total ion count; TIC). Table is available online in MS Excel format.

Supplemental Table S2b. Targeted metabolic proteome results grouped by enzyme pathway/complex. Table is available online in MS Excel format.

SI References

1. Subudhi, A. W., Bourdillon, N., Bucher, J., Davis, C., Elliott, J. E., Eutermoster, M., Evero, O., Fan, J. L., Jameson-Van Houten, S., Julian, C. G., Kark, J., Kark, S., Kayser, B., Kern, J. P., Kim, S. E., Lathan, C., Laurie, S. S., Lovering, A. T., Paterson, R., Polaner, D. M., Ryan, B. J., Spira, J. L., Tsao, J. W., Wachsmuth, N. B., and Roach, R. C. (2014) AltitudeOmics: the integrative physiology of human acclimatization to hypobaric hypoxia and its retention upon reascent. *PLoS One* **9**, e92191
2. Amann, M., Goodall, S., Twomey, R., Subudhi, A. W., Lovering, A. T., and Roach, R. C. (2013) AltitudeOmics: on the consequences of high-altitude acclimatization for the development of fatigue during locomotor exercise in humans. *Journal of applied physiology* **115**, 634-642
3. Fan, J. L., Subudhi, A. W., Evero, O., Bourdillon, N., Kayser, B., Lovering, A. T., and Roach, R. C. (2014) AltitudeOmics: enhanced cerebrovascular reactivity and ventilatory response to CO2 with high-altitude acclimatization and reexposure. *Journal of applied physiology* **116**, 911-918
4. Goodall, S., Twomey, R., Amann, M., Ross, E. Z., Lovering, A. T., Romer, L. M., Subudhi, A. W., and Roach, R. C. (2014) AltitudeOmics: exercise-induced supraspinal fatigue is attenuated in healthy humans after acclimatization to high altitude. *Acta physiologica* **210**, 875-888
5. Ryan, B. J., Wachsmuth, N. B., Schmidt, W. F., Byrnes, W. C., Julian, C. G., Lovering, A. T., Subudhi, A. W., and Roach, R. C. (2014) AltitudeOmics: rapid hemoglobin mass alterations with early acclimatization to and de-acclimatization from 5260 m in healthy humans. *PloS one* **9**, e108788
6. Subudhi, A. W., Fan, J. L., Evero, O., Bourdillon, N., Kayser, B., Julian, C. G., Lovering, A. T., Panerai, R. B., and Roach, R. C. (2014) AltitudeOmics: cerebral autoregulation during ascent, acclimatization, and re-exposure to high altitude and its relation with acute mountain sickness. *Journal of applied physiology* **116**, 724-729
7. Subudhi, A. W., Fan, J. L., Evero, O., Bourdillon, N., Kayser, B., Julian, C. G., Lovering, A. T., and Roach, R. C. (2014) AltitudeOmics: effect of ascent and acclimatization to 5260 m on regional cerebral oxygen delivery. *Experimental physiology* **99**, 772-781

8. D'Alessandro, A., Nemkov, T., Sun, K., Liu, H., Song, A., Monte, A. A., Subudhi, A. W., Lovering, A. T., Dvorkin, D., Julian, C. G., Kevil, C. G., Kolluru, G. K., Shiva, S., Gladwin, M. T., Xia, Y., Hansen, K. C., and Roach, R. C. (2016) AltitudeOmics: Red Blood Cell Metabolic Adaptation to High Altitude Hypoxia. *Journal of proteome research* **15**, 3883-3895
9. Liu, H., Zhang, Y., Wu, H., D'Alessandro, A., Yegutkin, G. G., Song, A., Sun, K., Li, J., Cheng, N. Y., Huang, A., Edward Wen, Y., Weng, T. T., Luo, F., Nemkov, T., Sun, H., Kellems, R. E., Karmouty-Quintana, H., Hansen, K. C., Zhao, B., Subudhi, A. W., Jameson-Van Houten, S., Julian, C. G., Lovering, A. T., Eltzschig, H. K., Blackburn, M. R., Roach, R. C., and Xia, Y. (2016) Beneficial Role of Erythrocyte Adenosine A2B Receptor-Mediated AMP-Activated Protein Kinase Activation in High-Altitude Hypoxia. *Circulation* **134**, 405-421
10. Song, A., Zhang, Y., Han, L., Yegutkin, G. G., Liu, H., Sun, K., D'Alessandro, A., Li, J., Karmouty-Quintana, H., Iriyama, T., Weng, T., Zhao, S., Wang, W., Wu, H., Nemkov, T., Subudhi, A. W., Jameson-Van Houten, S., Julian, C. G., Lovering, A. T., Hansen, K. C., Zhang, H., Bogdanov, M., Dowhan, W., Jin, J., Kellems, R. E., Eltzschig, H. K., Blackburn, M., Roach, R. C., and Xia, Y. (2017) Erythrocytes retain hypoxic adenosine response for faster acclimatization upon re-ascent. *Nature communications* **8**, 14108
11. Sun, K., Zhang, Y., D'Alessandro, A., Nemkov, T., Song, A., Wu, H., Liu, H., Adebiyi, M., Huang, A., Wen, Y. E., Bogdanov, M. V., Vila, A., O'Brien, J., Kellems, R. E., Dowhan, W., Subudhi, A. W., Jameson-Van Houten, S., Julian, C. G., Lovering, A. T., Safo, M., Hansen, K. C., Roach, R. C., and Xia, Y. (2016) Sphingosine-1-phosphate promotes erythrocyte glycolysis and oxygen release for adaptation to high-altitude hypoxia. *Nature communications* **7**, 12086
12. Dreyer, H. C., Fujita, S., Cadenas, J. G., Chinkes, D. L., Volpi, E., and Rasmussen, B. B. (2006) Resistance exercise increases AMPK activity and reduces 4E-BP1 phosphorylation and protein synthesis in human skeletal muscle. *The Journal of physiology* **576**, 613-624
13. Gnaiger, E. (2009) Capacity of oxidative phosphorylation in human skeletal muscle: new perspectives of mitochondrial physiology. *The international journal of biochemistry & cell biology* **41**, 1837-1845
14. Pesta, D., and Gnaiger, E. (2012) High-resolution respirometry: OXPHOS protocols for human cells and permeabilized fibers from small biopsies of human muscle. *Methods in molecular biology* **810**, 25-58
15. Nesvizhskii, A. I., Keller, A., Kolker, E., and Aebersold, R. (2003) A statistical model for identifying proteins by tandem mass spectrometry. *Analytical chemistry* **75**, 4646-4658